



OPEN

Distributed time-varying out formation-containment tracking of multi-UAV systems based on finite-time event-triggered control

Xin Cai, Xiaozhou Zhu & Wen Yao

Considering the limited communication resources and slow convergence speed of multi-unmanned aerial vehicle (UAV) systems, this paper presents a finite-time even-triggered control framework for multi-UAV systems to achieve formation-containment tracking control. First, a virtual leader with time-varying output is introduced so that the trajectory of the whole system can be manipulated in real time. Second, the finite-time control enables that the systematic error converge to a small neighborhood of origin in finite time. Third, in order to save communication resources, an event-triggering function is developed to generate the control event sequences, which avoids continuous update of the controller. Rigorous proof shows the finite-time stability of the proposed control algorithm, and Zeno behavior is strictly excluded for each UAV. Finally, some numerical simulations are given to verify the effectiveness of the proposed controllers.

In recent decades, cooperative control of multi-UAV systems has become a hot research topic due to its wide application of load transportation, localization and other fields¹⁻⁵. Cooperative control problems mainly includes leaderless consensus⁶, leader-following tracking^{7,8}, formation^{9,10} and containment^{11,12}. Das et al.¹³ and Fax and Murray¹⁴ described several methods of formation control, Ge et al.¹⁵ studied formation tracking control problem based on potential field, took the average position of all agents as virtual leaders, and transformed the task into controlling virtual leaders to track the center of the desired formation. In addition to the formation control problem, containment control also attract the attention of many people. The goal of containment control is to drive all followers to enter the convex hull formed by the leaders¹⁶. In¹⁷, the containment control of the multi-agent system under switched topology was discussed. Haghshenas et al.¹⁸ solved the containment control problem of heterogeneous linear multi-agent systems.

Inspired by the containment control and the formation control, a more complicated formation-containment problem arises, where the leaders need to accomplish a desired formation and the followers are required to converge to the convex hull spanned by the leaders simultaneously. Liu et al.¹⁹ considered the influence of control input with time delay on formation-containment control of multi-agent system. Han et al.²⁰ and Dong et al.²¹ designed the formation-containment control protocol for second-order and high-order multi-agent systems, and used a Riccati equation to solve the gain matrix in the control protocol. In²², for the multi-agent system with uncertain nonlinear dynamics and directed communication constraints, a distributed adaptive control approach was proposed to complete the formation-containment target.

It should be pointed out that the macroscopic movement of the whole system cannot be controlled effectively and flexibly in the above formation-containment works¹⁹⁻²². In the cooperative transportation application of a group of UAVs crossing dangerous areas, in addition to completing the task of formation-containment, the multi-UAV system should also track the desired trajectory so that all the UAVs can avoid the dangerous area and reach the destination safely. Therefore, the problem of formation-containment tracking appears. In^{23,24}, the formation-containment tracking problem was solved for high-order multi-agent system. It can be seen that consensus tracking problem, containment problem and formation problem are special cases of formation-containment

Defense Innovation Institute, Chinese Academy of Military Science, Beijing 100000, China. email: wendy0782@126.com

tracking problem²³. How to make the whole system move flexibly and effectively is a challenge to enable it to cope with complex real environments.

It is worth noting that most of the existing research focuses on the asymptotic convergence of multi-agent systems^{20,25}. In practical applications, multi-UAV systems require fast response. Compared with the asymptotic convergence algorithm, the finite-time control protocol has faster convergence speed and better anti-interference ability, therefore, it is necessary to study the finite-time control of multi-agent systems. In⁹, the finite-time time-varying formation tracking problem of multi-agent systems was studied in directed topology. A finite-time formation tracking protocol was provided in the presence of mismatched disturbances for high-order multi-agent systems in²⁶. Yu et al.¹¹ developed a distributed finite-time sliding mode observer for estimating the reference for each UAV, and designed a finite-time containment controller. Nevertheless, these studies only consider formation tracking problem or containment control separately, but do not solve the problem of formation-containment. Namely, it is not guaranteed to complete the formation-containment tracking task in the finite time.

Furthermore, it should be pointed out that the above finite-time controllers employ the continuous time control method, which means that the controller needs to constantly update its control input. However, in practical applications, UAVs are usually equipped with embedded microprocessors with limited computing resources. In view of this concern, event-triggered control is developed to avoid the controller being constantly updated^{27–29}. In¹, aiming at the collaborative transportation problem of the multi-UAV system, a self-triggered method was designed to lower the communication frequency. Chen et al.³⁰ discussed the event-triggered formation-containment problem of Euler Lagrange system. In³¹, the formation control problem of the multi-UAV system was considered through a dynamic event-triggered control algorithm, which includes a dynamic threshold. Combining event-triggered control with existing cooperative control is of great value to multi-agent coordinated control problems. The main challenge of event-triggered control is to design triggering functions according to different task scenarios to ensure convergence, and not Zeno behavior occurs.

Motivated by challenges stated above, considering both the limited communication resources and slow convergence speed of the multi-UAV system, this paper investigates the finite-time event-triggered formation-containment tracking control for the multi-UAV system. Compared with the existing literature, the main contributions of this paper are summarized as follows.

- a virtual leader with time-varying output is introduced so that the trajectory of the whole system can be manipulated in real time
- The distributed finite-time protocols are utilized to ensure that the multi-UAV system realize the expected formation-containment tracking in finite time. The upper bound of settling time is given by carefully constructing the Lyapunov function.
- The event-triggering function is developed in the multi-UAV system, which avoids the continuous update input of the controller and greatly reduces the dependence on communication resources.

The remaining sections of this paper are organized as follows. In “[Preliminaries and problem formulation](#)”, some basic preliminaries and problem formulation are introduced. “[Formation-containment tracking protocol design](#)” presents the designs of formation-containment tracking protocol and analyzes the stability of the system. The results of simulation experiments are provided in “[Simulation results](#)”. Finally, the conclusion is drawn in “[Conclusions](#)”.

Notations: For $\mathbf{x} = [x_1, x_2, \dots, x_n]^T$ and a positive constant α , we define $\text{sig}(\mathbf{x})^\alpha = [\text{sgn}(x_1)|x_1|^\alpha, \text{sgn}(x_2)|x_2|^\alpha, \dots, \text{sgn}(x_n)|x_n|^\alpha]^T$, where $\text{sgn}(\cdot)$ is the signum function. Let $\|\cdot\|$ and $\text{diag}\{\dots\}$ represent the 2-norm, the block-diagonal matrix. \otimes is the Kronecker product. \mathbb{R}^n , \mathbf{I}_n , $\mathbf{0}_n$ denote $n \times 1$ real vectors, $n \times n$ identity matrices and $n \times 1$ zero vectors, respectively. $\lambda_{\min}(\cdot)$, $\lambda_{\max}(\cdot)$ represent the maximum and minimum eigenvalues of the square matrix, respectively.

Preliminaries and problem formulation

Graph theory and lemmas. A directed graph $G = (V, E, A)$ is used to represent the information interaction relationship of multi-UAV system. $V = \{1, 2, \dots, n\}$ is the set of nodes in graph G . E is the set of edges in the graph. In a directed graph, each edge can only represent one-way information transmission. $(i, j) \in E$ only indicates that nodes i can transfer information to nodes j , and $(i, j) \in E \not\Rightarrow (j, i) \in E$. $A = [a_{ij}]_{n \times n}$ is the weighted adjacency matrix of the graph, if there exists an edge between the node i and node j , namely, $(i, j) \in E$, then, $a_{ij} = 1$, otherwise $a_{ij} = 0$. Define the degree matrix as $D = \text{diag}[d_{11}, \dots, d_{nn}]$ with $\sum_{j=1}^n a_{ij}$ and the Laplacian matrix of G is defined as $L = D - W$. A directed graph is said to have a spanning tree if there exists at least one node having a directed path to all the other nodes, and that node is called the root node.

The multi-UAV system is represented by three layers, as shown in Fig. 1. The inner layer consists of followers, the real leaders constitute the outer layer, and the guidance layer consists of virtual leader. The inner layer and the outer layer jointly complete the containment task, and the formation tracking target is accomplished by the cooperation of the guidance layer and the outer layer. Assume that the information exchange between two adjacent layers is unidirectional and the information interaction between each agent in the layer is bidirectional. The system consists of $1 + N + M$ agents, where $i = 0$ represents agent of the guidance layer, namely the virtual leader, $E = \{1, 2, \dots, N\}$ are the index of the real leaders, which constitute outer layer, and the index set of followers in the inner layer are $F = \{N + 1, N + 2, \dots, N + M\}$, then the Laplace matrix $L_A \in \mathbb{R}^{(N+M+1) \times (N+M+1)}$ of the communication topology G_A is expressed in the following form:

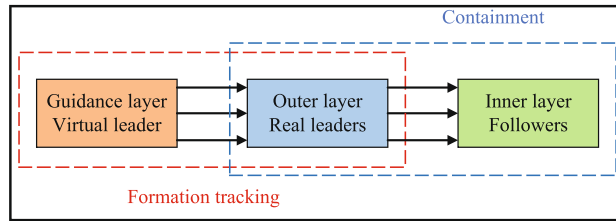


Figure 1. Three-layer structure representation.

$$L_A = \begin{bmatrix} 0 & 0_{1 \times N} & 0_{1 \times M} \\ L_{12} & L_1 & 0_{N \times M} \\ 0_{M \times 1} & L_2 & L_3 \end{bmatrix}$$

where $L_{12} \in \mathbb{R}^{N \times 1}, L_1 \in \mathbb{R}^{N \times N}, L_2 \in \mathbb{R}^{M \times N}, L_3 \in \mathbb{R}^{M \times M}$.

Define $B = \text{diag}\{L_{12}^T\}$, and $L = L_1 - B$ describes communication topology between real leaders without receiving information from the virtual leader. L_2 expresses the communication from real leaders to followers. L_3 denotes the communication between followers.

Lemma 1 ³²If exists, $\delta_1, \delta_2, c > 0, p, q > 1$ and $\frac{1}{p} + \frac{1}{q} = 1$, then $\delta_1 \delta_2 \leq c^p \frac{\delta_1^p}{p} + c^{-q} \frac{\delta_2^q}{q}$.

Lemma 2 ³³For $x_i \in \mathbb{R}$, if $\alpha \in [1, +\infty)$, then $(\sum_{i=1}^n |x_i|)^\alpha \geq \sum_{i=1}^n |x_i|^\alpha \geq n^{1-\alpha} (\sum_{i=1}^n |x_i|)^\alpha$; and if exists $\alpha \in (0, 1]$, then $(\sum_{i=1}^n |x_i|)^\alpha \leq \sum_{i=1}^n |x_i|^\alpha \leq n^{1-\alpha} (\sum_{i=1}^n |x_i|)^\alpha$.

Lemma 3 ³⁴Consider the system $\dot{x} = f(x), x \in \mathbb{R}^n$, if there exists a continuous differentiable function $V: [0, \infty) \rightarrow [0, \infty)$, and it satisfies $\dot{V}(x) \leq -c(V(x))^\eta$, where $c > 0$ and $0 < \eta < 1$. The system can be stabilized in a finite time, and the finite settling time satisfies $T \leq (V(x_0))^{1-\eta} / c(1 - \eta)$.

Assumption 1 The topology between the real leaders and the virtual leader contains a spanning tree, and the root node of the spanning tree is the virtual leader.

Assumption 2 The communication topology between followers is a directed graph, and for each follower, there exists at least one directed path from the real leader to the follower.

Multi-UAV formation-containment tracking problem formulation. For each UAV in the multi-UAV system, the controller design can be divided into inner-loop control and outer-loop control. The inner loop mainly completes the stabilization of the attitude, while the outer loop realizes the tracking of the given trajectory. This paper is mainly concerned with the formation-containment tracking problem of the outer-loop. Define $p_i(t) = [x_i, y_i, z_i]^T$, then the outer-loop dynamic model of each UAV can be described as follows³⁵:

$$\begin{cases} \dot{p}_i = v_i \\ m_i \dot{v}_i = -T_{\tau_i} R_i e_3 + m_i g e_3 \end{cases} \quad i = 1, 2, \dots, n \tag{1}$$

where $p_i \in \mathbb{R}^3, v_i \in \mathbb{R}^3$ and $R_i \in \mathbb{R}^{3 \times 3}$ represents the position, velocity and rotation matrix of each UAV, $e_3 = [0, 0, 1]^T, T_{\tau_i}$ represents the total lift, m_i, g are the mass of the UAV and gravitational acceleration, respectively. Define the control input vector of each UAV $u_i = -\frac{T_{\tau_i}}{m_i} R_i e_3 + g e_3$, then the dynamic model of the UAV (1) can be rewritten by the following double integrator in³⁶,

$$\begin{cases} \dot{p}_i(t) = v_i(t) \\ \dot{v}_i(t) = u_i(t) \end{cases} \tag{2}$$

Denote $\chi_i = [p_i^T, v_i^T]^T, o_i$ represents the position offset vector between the real leaders and the virtual leader.

Definition 1 If for all real leaders and any given initial states,

$$\begin{aligned} \lim_{t \rightarrow T_1} \|p_i(t) - o_i - p_0(t)\| &= 0 \\ \lim_{t \rightarrow T_1} \|v_i(t) - v_0(t)\| &= 0 \quad i \in E \end{aligned} \tag{3}$$

then in a finite time T_1 , all the real leaders achieve the expected formation described by o_i .

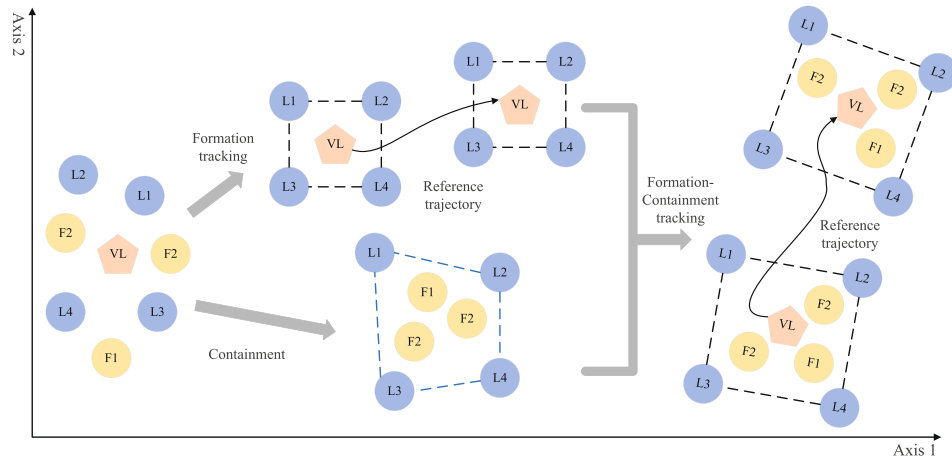


Figure 2. Formation-containment tracking.

Definition 2 For each follower, if there exists $T_2 > 0$ and non negative constants ϖ_{ij} satisfying $\sum_{i=1}^N \varpi_{ij} = 1$ such that

$$\lim_{t \rightarrow T_2} \left\| \chi_j(t) - \sum_{i=1}^N \varpi_{ij} \chi_i(t) \right\| = 0, \forall j \in F, \forall i \in E \tag{4}$$

then followers is said to achieve containment in a finite time T_2 .

Definition 3 If both the conditions (3) and (4) are established at the same time, namely, a desired formation is formed between real leaders in a finite time T_1 , the followers converge to the convex hull constructed by the real leaders in a finite time T_2 , and then Multi-UAV system realizes the finite-time formation-containment tracking, as shown in Fig. 2.

Therefore, the principal problem to be studied in this paper can be expressed as follows: for the UAV system described in (2), design control laws for leaders and followers to achieve the formation-containment tracking goal defined in Definition 3.

Formation-containment tracking protocol design

Finite-time event-triggered formation tracking control for leaders. It is worth noting that only real leaders directly connected to the virtual leader can receive virtual leader’s states, therefore, a distributed fixed time observer is designed for each real leader to estimate the state of virtual leader.

$$\begin{aligned} \ddot{\hat{p}}_i &= \frac{\sum_{j=0}^N a_{ij} \ddot{\hat{p}}_j}{\sum_{j=0}^N a_{ij}} - \frac{\alpha}{\sum_{j=0}^N a_{ij}} \text{sig} \left(\sum_{j=0}^N a_{ij} (\hat{p}_i - \hat{p}_j) \right)^{a/b} \\ &\quad - \frac{\beta}{\sum_{j=0}^N a_{ij}} \text{sig} \left(\sum_{j=0}^N a_{ij} (\dot{\hat{p}}_i - \dot{\hat{p}}_j) \right)^{c/d} \end{aligned} \quad i \in E \tag{5}$$

where $\alpha > 0, \beta > 0, a, b, c, d$ are positive odd integers satisfying $a > b, c < d, \dot{\hat{p}}_0 = v_0, \hat{p}_i$ represents the estimated velocity of the i_{th} UAV. Under Assumption 1, the observer can estimate the state value in a fixed time³⁷.

$$T < \frac{b}{\alpha(a-b)(3N)^{(1-a/b)/2}} + \frac{d}{\beta(d-c)} \tag{6}$$

Remark 1 When $t \geq T$, we can conclude that $\hat{p}_1 = \hat{p}_2 = \dots = \hat{p}_N = \dot{p}_0 = v_0$. By further derivation, we get $\ddot{\hat{p}}_1 = \ddot{\hat{p}}_2 = \dots = \ddot{\hat{p}}_N = \ddot{p}_0 = u_0$.

Describe $\{t_0^i = 0, t_1^i, \dots, t_k^i, t_{k+1}^i, \dots\}$ as the trigger time sequence of i_{th} UAV. The finite-time event-triggered formation tracking controller is designed as follows:

$$\begin{aligned}
 u_i = & \ddot{\tilde{p}}_i(t_k^i) - k_1 \text{sig} \left[\sum_{j=1}^N a_{ij} ((p_i(t_k^i) - o_i) \right. \\
 & \left. - (p_j(t_k^i) - o_j)) + a_{i0} (p_i(t_k^i) - o_i) \right] \quad i \in E \\
 & - p_0(t_k^i)]^{\alpha_1} - k_2 \text{sig} \left[\sum_{j=1}^N a_{ij} (v_i(t_k^i) - v_j(t_k^i)) \right. \\
 & \left. - a_{i0} (v_i(t_k^i) - v_0(t_k^i)) \right]^{\alpha_2}
 \end{aligned} \tag{7}$$

where $k_1, k_2 > 0, 0 < \alpha_1 < 1, \alpha_2 = 2\alpha_1/(1 + \alpha_1)$.

Define the combinational tracking error as:

$$\begin{aligned}
 r_i(t) = & \sum_{j=1}^N a_{ij} ((p_i(t) - o_i) - (p_j(t) - o_j)) \\
 & + a_{i0} (p_i(t) - o_i - p_0(t)) \\
 q_i(t) = & \sum_{j=1}^N a_{ij} (v_i(t) - v_j(t)) + a_{i0} (v_i(t) - v_0(t))
 \end{aligned} \tag{8}$$

Define $R = [r_1^T, \dots, r_N^T]^T, Q = [q_1^T, \dots, q_N^T]^T$, where $r_i = [r_{i1}, r_{i2}, r_{i3}]^T, q_i = [q_{i1}, q_{i2}, q_{i3}]^T$. Define the tracking errors as: $\tilde{p}_i = p_i(t) - o_i - p_0(t), \tilde{v}_i = v_i(t) - v_0(t)$. The measurement errors are defined as follows:

$$\begin{aligned}
 \varphi_i^r = & \text{sig}(r_i(t_k^i))^{\alpha_1} - \text{sig}(r_i(t))^{\alpha_1} \\
 \varphi_i^q = & \text{sig}(q_i(t_k^i))^{\alpha_2} - \text{sig}(q_i(t))^{\alpha_2} \\
 \varphi_i^c = & \ddot{\tilde{p}}_i(t_k^i) - u_0(t)
 \end{aligned} \tag{9}$$

where $\varphi_i^r = [\varphi_{i1}^r, \varphi_{i2}^r, \varphi_{i3}^r]^T, \varphi_i^q = [\varphi_{i1}^q, \varphi_{i2}^q, \varphi_{i3}^q]^T, \varphi_i^c = [\varphi_{i1}^c, \varphi_{i2}^c, \varphi_{i3}^c]^T$

Define $\tilde{P} = [\tilde{p}_1^T, \dots, \tilde{p}_N^T]^T, \tilde{V} = [\tilde{v}_1^T, \dots, \tilde{v}_N^T]^T$ where $\tilde{p}_i = [\tilde{p}_{i1}, \tilde{p}_{i2}, \tilde{p}_{i3}]^T, \tilde{v}_i = [\tilde{v}_{i1}, \tilde{v}_{i2}, \tilde{v}_{i3}]^T$, then we can get $R = L_1 \otimes \mathbf{I}_3 \tilde{P}$ and $Q = L_1 \otimes \mathbf{I}_3 \tilde{V}$. According Remark 1, combine (7), (8) and (9), the system error equation can be described as follows:

$$\begin{aligned}
 \dot{R} = & Q \\
 \dot{Q} = & - (L_1 \otimes \mathbf{I}_3) (k_1 \text{sig}(R)^{\alpha_1} + k_2 \text{sig}(Q)^{\alpha_2} \\
 & + k_1 \varphi^r + k_2 \varphi^q)
 \end{aligned} \tag{10}$$

where $\varphi^r = [(\varphi_1^r)^T, (\varphi_2^r)^T, \dots, (\varphi_N^r)^T]^T, \varphi^q = [(\varphi_1^q)^T, (\varphi_2^q)^T, \dots, (\varphi_N^q)^T]^T$.

Theorem 1 Let Assumption 1 hold, then the multi-UAV system (2) can achieve the desired formation in finite time under the protocol (7) and trigger function (11). If exists $0 < \alpha_1 < 1, \alpha_2 = 2\alpha_1/(1 + \alpha_1), 1 - 3 \frac{1-\alpha_2}{2} \xi > 0, k_1 > k_2(3N) \frac{1-\alpha_1}{2(1+\alpha_1)} (\xi + N) \frac{c^{1+\alpha_1}}{1+\alpha_1}, k_1 > 2 \frac{2(1+\alpha_1)}{3+\alpha_1} \left(\sqrt{\frac{2}{\lambda_{\min}(L_1)}} \cdot \frac{\theta \lambda_{\max}(L_1)(1+\alpha_1)}{3+\alpha_1} \right)^{1+\alpha_1} (1 + \alpha_1) \frac{1-\alpha_1}{3+\alpha_1}, \frac{k_2(3+\alpha_1)}{2(1+\alpha_1)} (1 - 3 \frac{1-\alpha_2}{2} \xi) \left(\frac{\lambda_{\min}(L_1)}{2} \right) \frac{1-\alpha_1}{2(1+\alpha_1)} > \theta k_2(3N) \frac{1-\alpha_1}{2(1+\alpha_1)} (\xi + N) \frac{\alpha_1 c}{1+\alpha_1} + \theta \lambda_{\max}(L_1)$, where $c, \theta > 0$, the distributed event-triggered function is designed as follows:

$$t_i(t) = \|k_1 \varphi_i^r(t)\| + \|k_2 \varphi_i^q(t)\| - \xi \|\text{sig}(q_i(t))^{\alpha_2}\| \tag{11}$$

where $\xi \in (0, 1)$.

Proof The Lyapunov candidate is constructed as follows :

$$V_1(t) = k_1 \sum_{i=1}^N \sum_{j=1}^3 \frac{|x|^{\alpha_1+1}}{\alpha_1 + 1} (r_{ij}) + \frac{1}{2} Q^T (L_1^{-1} \otimes \mathbf{I}_3) Q \tag{12}$$

The derivative of (12) can be obtained:

$$\begin{aligned}
 \dot{V}_1(t) &= k_1 \sum_{i=1}^N \sum_{j=1}^3 \text{sig}(r_{ij})^{\alpha_1} \dot{r}_{ij} + Q^T L_1^{-1} \otimes \mathbf{I}_3 \dot{Q} \\
 &\quad - k_2 \sum_{i=1}^N q_i^T \text{sig}(q_i)^{\alpha_2} - \sum_{i=1}^N q_i^T (k_1 \phi_i^r + k_2 \phi_i^q) \\
 &\leq \sum_{i=1}^N \|q_i\| (\|k_1 \phi_i^r\| + \|k_2 \phi_i^q\|) - k_2 \sum_{i=1}^N q_i^T \text{sig}(q_i)^{\alpha_2} \\
 &\leq \xi k_2 \sum_{i=1}^N \|q_i\| \|\text{sig}(q_i)^{\alpha_2}\| - k_2 \sum_{i=1}^N q_i^T \text{sig}(q_i)^{\alpha_2} \\
 &\leq -k_2 \left(1 - 3^{\frac{1-\alpha_2}{2}} \xi\right) \sum_{i=1}^N \|q_i\|^{\alpha_2+1}
 \end{aligned} \tag{13}$$

According to $k_2 > 0, 1 - 3^{\frac{1-\alpha_2}{2}} \xi > 0$, it can be concluded that $\dot{V}_1(t) < 0$ and the error system (10) is asymptotically stable.

To further prove that the system converges in finite time, the following Lyapunov function is constructed:

$$V(t) = V_1(t)^{\frac{3+\alpha_1}{2(1+\alpha_1)}} + \theta R^T (L_1^{-1} \otimes \mathbf{I}_3) Q \tag{14}$$

where θ is a positive constant, according to Lemmas 1 and 2, the following formula can be obtained

$$\begin{aligned}
 V_1(t)^{\frac{3+\alpha_1}{2(1+\alpha_1)}} &\geq \left(k_1 \sum_{i=1}^N \sum_{j=1}^3 \int_0^{r_{ij}} \text{sig}(x)^{\alpha_1} dx \right)^{\frac{3+\alpha_1}{2(1+\alpha_1)}} + \left(\frac{1}{2} Q^T (L_1^{-1} \otimes \mathbf{I}_3) Q \right)^{\frac{3+\alpha_1}{2(1+\alpha_1)}} \\
 &\geq \left(\frac{k_1}{1 + \alpha_1} \sum_{i=1}^N \sum_{j=1}^3 |r_{ij}|^{\alpha_1+1} \right)^{\frac{3+\alpha_1}{2(1+\alpha_1)}} + \left(\frac{\lambda_{\min}(L_1)}{2} \|Q\|^2 \right)^{\frac{3}{2(1+\alpha_1)}} \\
 &\geq \left(\frac{k_1}{1 + \alpha_1} \|R\|^{1+\alpha_1} \right)^{\frac{3+\alpha_1}{2(1+\alpha_1)}} + \left(\frac{\lambda_{\min}(L_1)}{2} \|Q\|^2 \right)^{\frac{3+\alpha_1}{2(1+\alpha_1)}}
 \end{aligned} \tag{15}$$

$$\begin{aligned}
 \theta R^T (L_1^{-1} \otimes \mathbf{I}_3) Q &\geq -\theta \lambda_{\max}(L_1) \|R\| \|Q\| \\
 &\geq -\theta \lambda_{\max}(L_1) \left(\frac{2}{3 + \alpha_1} h^{\frac{3+\alpha_1}{2}} \|R\|^{\frac{3+\alpha_1}{2}} + \frac{1 + \alpha_1}{3 + \alpha_1} h^{-\frac{3+\alpha_1}{1+\alpha_1}} \|Q\|^{\frac{3+\alpha_1}{1+\alpha_1}} \right)
 \end{aligned} \tag{16}$$

where h is a positive constant, combining (15) and (16),

$$\begin{aligned}
 V(t) &\geq \left(\left(\frac{k_1}{1 + \alpha_1} \right)^{\frac{3(1+\alpha_1)}{2(1+\alpha_1)}} - \frac{2\theta \lambda_{\max}(L_1)}{3 + \alpha_1} h^{\frac{3+\alpha_1}{2}} \right) \|R\|^{\frac{3+\alpha_1}{2}} \\
 &\quad + \left(\frac{\lambda_{\min}(L_1)}{2} - \frac{\theta \lambda_{\max}(L_1)(1 + \alpha_1)}{3 + \alpha_1} h^{-\frac{3+\alpha_1}{1+\alpha_1}} \right) \|Q\|^{\frac{3+\alpha_1}{1+\alpha_1}}
 \end{aligned} \tag{17}$$

In order to ensure that $V(t)$ is positive definite, satisfying

$$k_1 > 2^{\frac{2(1+\alpha_1)}{3+\alpha_1}} \left(\sqrt{\frac{2}{\lambda_{\min}(L_1)} \frac{\theta \lambda_{\max}(L_1)(1 + \alpha_1)}{3 + \alpha_1}} \right)^{1+\alpha_1} (1 + \alpha_1)^{\frac{1-\alpha_1}{3+\alpha_1}}$$

Further, taking the derivative of $V(t)$

$$\begin{aligned}
 \dot{V}(t) &= \frac{3 + \alpha_1}{2(1 + \alpha_1)} V_1(t)^{\frac{1-\alpha_1}{2(1+\alpha_1)}} \dot{V}_1(t) + \theta Q^T (L_1^{-1} \otimes \mathbf{I}_3) Q \\
 &\quad + \theta R^T (L_1^{-1} \otimes \mathbf{I}_3) \dot{Q} \\
 &\leq -\frac{k_2(3 + \alpha_1)}{2(1 + \alpha_1)} \left(1 - 3^{\frac{1-\alpha_2}{2}} \xi\right) \left(\frac{\lambda_{\min}(L_1)}{2}\right)^{\frac{1-\alpha_1}{2(1+\alpha_1)}} \|Q\|^2 \\
 &\quad + \theta \lambda_{\max}(L_1) \|Q\|^2 - \theta k_1 \|R\|^{\alpha_1+1} \\
 &\quad + \theta k_2 (3N)^{\frac{1-\alpha_1}{2(1+\alpha_1)}} (\xi + N) \|R\| \|Q\|^{\alpha_2} \\
 &\leq -\left(\theta k_1 - \theta k_2 (3N)^{\frac{1-\alpha_1}{2(1+\alpha_1)}} (\xi + N) \frac{c^{1+\alpha_1}}{1 + \alpha_1}\right) \|R\|^{\alpha_1+1} \\
 &\quad - \left(\frac{k_2(3 + \alpha_1)}{2(1 + \alpha_1)} \left(1 - 3^{\frac{1-\alpha_2}{2}} \xi\right) \left(\frac{\lambda_{\min}(L_1)}{2}\right)^{\frac{1-\alpha_1}{2(1+\alpha_1)}} \right. \\
 &\quad \left. - \theta k_2 (3N)^{\frac{1-\alpha_1}{2(1+\alpha_1)}} (\xi + N) \frac{\alpha_1 c^{-\frac{1+\alpha_1}{\alpha_1}}}{1 + \alpha_1} - \theta \lambda_{\max}(L_1)\right) \|Q\|^2 \\
 &= -\omega_1 \|R\|^{\alpha_1+1} - \omega_2 \|Q\|^2 \\
 &\leq -\omega (\|R\|^{\alpha_1+1} + \|Q\|^2)
 \end{aligned} \tag{18}$$

where $c > 0, \omega = \min(\omega_1, \omega_2)$. From $\omega_1, \omega_2 > 0$, there exists $\dot{V}(t) < 0$.

Similarly, according to Lemmas 1 and 2, it can be obtained that:

$$\begin{aligned}
 V_1(t) &= \frac{3+\alpha_1}{2(1+\alpha_1)} \\
 &\leq 2^{\frac{1-\alpha_1}{2(1+\alpha_1)}} \left(\frac{k_1 N^{\frac{1-\alpha_1}{2}}}{1 + \alpha_1}\right)^{\frac{3+\alpha_1}{2(1+\alpha_1)}} \|R\|^{\frac{3+\alpha_1}{2}} \\
 &\quad + \frac{1}{2} \lambda_{\max}(L_1)^{\frac{3+\alpha_1}{2(1+\alpha_1)}} \|Q\|^{\frac{3+\alpha_1}{1+\alpha_1}}
 \end{aligned} \tag{19}$$

and

$$\begin{aligned}
 &\theta R^T (L_1^{-1} \otimes \mathbf{I}_3) Q \\
 &\leq \frac{2\theta \lambda_{\max}(L_1)}{3 + \alpha_1} h^{\frac{3+\alpha_1}{2}} \|R\|^{\frac{3+\alpha_1}{2}} \\
 &\quad + \frac{(1 + \alpha_1)\theta \lambda_{\max}(L_1)}{3 + \alpha_1} h^{-\frac{3+\alpha_1}{1+\alpha_1}} \|Q\|^{\frac{3+\alpha_1}{1+\alpha_1}}
 \end{aligned} \tag{20}$$

Combining (19) and (20), we get

$$\begin{aligned}
 V(t) &\leq \beta_1 \|R\|^{\frac{3+\alpha_1}{2}} + \beta_2 \|Q\|^{\frac{3+\alpha_1}{1+\alpha_1}} \\
 &\leq \beta \left(\|R\|^{\frac{3+\alpha_1}{2}} + \|Q\|^{\frac{3+\alpha_1}{1+\alpha_1}}\right)
 \end{aligned} \tag{21}$$

where $\beta = \max(\beta_1, \beta_2)$. Combining (18), and further obtain

$$\begin{aligned}
 \dot{V}(t) &\leq -\omega (\|R\|^{\alpha_1+1} + \|Q\|^2) \\
 &\leq -\omega \left(\|R\|^{\frac{3+\alpha_1}{2}} + \|Q\|^{\frac{3+\alpha_1}{1+\alpha_1}}\right)^{\frac{2(1+\alpha_1)}{3+\alpha_1}} \\
 &\leq -\omega \left(\frac{V(t)}{\beta}\right)^{\frac{2(1+\alpha_1)}{3+\alpha_1}}
 \end{aligned} \tag{22}$$

According to Lemma 3, the error system (10) satisfies the condition of finite time stability, namely, R and Q converge to origin in finite time, with the settling time $T_1 \leq \frac{\beta^{\frac{2(1+\alpha_1)}{3+\alpha_1}} (3+\alpha_1)}{\omega(1-\alpha_1)} V^{\frac{1-\alpha_1}{3+\alpha_1}}(0)$. Considering $R = (L_1 \otimes \mathbf{I}_3) \tilde{P}$

, $Q = (L_1 \otimes \mathbf{I}_3) \tilde{V}$ and L_1 is positive definite, we soon have $\tilde{p}_i = \tilde{v}_i = 0$ when $t \geq T_1$, which means that the desired formation is formed in a finite time T_1 . This completes the proof. \square

Theorem 2 Considering Assumption 1 holds and the conditions of Theorem 1 are satisfied, Zeno behavior can be excluded in the control protocol (7) and distributed triggering function (11) for multi-UAV systems.

Proof For $t \in [t_k^i, t_{k+1}^i)$, we derive

$$\begin{aligned} & \|k_1 \dot{\varphi}_i^r(t)\| + \|k_2 \dot{\varphi}_i^q(t)\| \\ &= \|k_1 \text{sig}(\dot{r}_i(t))^{\alpha_1}\| + \|k_2 \text{sig}(\dot{q}_i(t))^{\alpha_2}\| \\ &\leq k_1 3^{\frac{1-\alpha_1}{2}} \|q_i(t)\|^{\alpha_1} + k_2 3^{\frac{1-\alpha_2}{2}} \|\dot{q}_i(t)\|^{\alpha_2} \end{aligned} \tag{23}$$

when $t = t_k^i, \|\varphi_i^r(t_k^i)\| = 0, \|\varphi_i^q(t_k^i)\| = 0$, and then

$$\begin{aligned} & \|k_1 \varphi_i^r(t)\| + \|k_2 \varphi_i^q(t)\| \\ &= \int_{t_k^i}^t (\|k_1 \dot{\varphi}_i^r(t)\| + \|k_2 \dot{\varphi}_i^q(t)\|) dt \\ &\leq k_1 3^{\frac{1-\alpha_1}{2}} \int_{t_k^i}^t \|q_i(t)\|^{\alpha_1} dt + k_2 3^{\frac{1-\alpha_2}{2}} \int_{t_k^i}^t \|\dot{q}_i(t)\|^{\alpha_2} dt \\ &\leq 2\delta_1 \int_{t_k^i}^t \delta_2 dt = 2\delta_1 \delta_2 (t - t_k^i) \end{aligned} \tag{24}$$

where $\delta_1 = \max(3^{\frac{1-\alpha_1}{2}} k_1, 3^{\frac{1-\alpha_2}{2}} k_2), \delta_2 = \max(\|q_i(t)\|^{\alpha_1}, \|\dot{q}_i(t)\|^{\alpha_2})$. When $\|q_i\| = 0$, the formation has been formed, and the controller does not need to be updated. Zeno behavior is naturally excluded. when formation is not achieved, we get $\|q_i(t)\|^\alpha > 0$. According to the event-triggered function (11), we further obtain

$$\begin{aligned} 2\delta_1 \delta_2 (t_{k+1}^i - t_k^i) &\geq \|k_1 \varphi_i^r(t)\| + \|k_2 \varphi_i^q(t)\| \\ &> 3^{\frac{1-\alpha_2}{2}} \xi \|q_i\|^{\alpha_2} > 0 \end{aligned} \tag{25}$$

From (25), we get

$$t_{k+1}^i - t_k^i > \frac{3^{\frac{1-\alpha_2}{2}} \xi \|q_i\|^{\alpha_2}}{2\delta_1 \delta_2} > 0 \tag{26}$$

From (26), The inter-event interval has a strict positive lower bound and zeno behavior does not occur in the system. The proof is completed. \square

Finite-time event-triggered containment control for followers. Describe $t_0, t_1, \dots, t_k, \dots$ as the event trigger time series, where t_k denotes the k_{th} triggered time of followers. The finite-time event-triggered containment controller is designed as follows:

$$\begin{aligned} u_i(t) &= -k_3 \text{sig} \left[\sum_{j=1}^{N+M} a_{ij} (p_i(t_k^i) - p_j(t_k^i)) \right]^{\alpha_3} \\ &\quad - k_4 \text{sig} \left[\sum_{j=1}^{N+M} a_{ij} (v_i(t_k^i) - v_j(t_k^i)) \right]^{\alpha_4} \quad i \in F \end{aligned} \tag{27}$$

where $k_3, k_4 > 0, \alpha_3 \in (0, 1), \alpha_4 = \frac{2\alpha_3}{1+2\alpha_3}$.

The combinational tracking errors are defined as

$$\begin{aligned} \mathcal{E}_{p_i}(t) &= \sum_{j=1}^{N+M} a_{ij} (p_i(t) - p_j(t)) \\ \mathcal{E}_{v_i}(t) &= \sum_{j=1}^{N+M} a_{ij} (v_i(t) - v_j(t)) \quad i \in F \end{aligned} \tag{28}$$

Define $\mathcal{E}_p = [\mathcal{E}_{p_1}^T, \dots, \mathcal{E}_{p_M}^T]^T, \mathcal{E}_v = [\mathcal{E}_{v_1}^T, \dots, \mathcal{E}_{v_M}^T]^T$, where $\mathcal{E}_{p_i} = [\mathcal{E}_{p_{i1}}, \dots, \mathcal{E}_{p_{i3}}]^T, \mathcal{E}_{v_i} = [\mathcal{E}_{v_{i1}}, \dots, \mathcal{E}_{v_{i3}}]^T$. Define the tracking errors as

$$\begin{cases} \tilde{\varepsilon}_{p_i} = p_i(t) - p_\tau(t) \\ \tilde{\varepsilon}_{v_i} = v_i(t) - v_\tau(t) \end{cases} \tag{29}$$

where $\tau \in E$ being the real leader directly connected to the followers. Define $\tilde{\mathcal{E}}_p = [\tilde{\varepsilon}_{p1}^T, \dots, \tilde{\varepsilon}_{pM}^T]^T$, $\tilde{\mathcal{E}}_v = [\tilde{\varepsilon}_{v1}^T, \dots, \tilde{\varepsilon}_{vM}^T]^T$, where $\tilde{\varepsilon}_{pi} = [\tilde{\varepsilon}_{pi1}, \tilde{\varepsilon}_{pi2}, \tilde{\varepsilon}_{pi3}]^T$, $\tilde{\varepsilon}_{vi} = [\tilde{\varepsilon}_{vi1}, \tilde{\varepsilon}_{vi2}, \tilde{\varepsilon}_{vi3}]^T$ then we get $\mathcal{E}_p = L_3 \otimes \mathbf{I}_3 \tilde{\mathcal{E}}_p$, $\mathcal{E}_v = L_3 \otimes \mathbf{I}_3 \tilde{\mathcal{E}}_v$. Define the measurement errors as

$$\begin{aligned} \zeta_i^p &= \text{sig}(\mathcal{E}_{pi}(t_k^i))^{\alpha_3} - \text{sig}(\mathcal{E}_{pi}(t))^{\alpha_3} \\ \zeta_i^v &= \text{sig}(\mathcal{E}_{vi}(t_k^i))^{\alpha_4} - \text{sig}(\mathcal{E}_{vi}(t))^{\alpha_4} \end{aligned} \tag{30}$$

where $\zeta_i^p = [\zeta_{i1}^p, \zeta_{i2}^p, \zeta_{i3}^p]^T$, $\zeta_i^v = [\zeta_{i1}^v, \zeta_{i2}^v, \zeta_{i3}^v]^T$. Combining (27), (28) and (30), the dynamic model of the Multi-UAV system can be rewritten as

$$\begin{aligned} \dot{\mathcal{E}}_p &= \mathcal{E}_v \\ \dot{\mathcal{E}}_v &= -(L_3 \otimes \mathbf{I}_3)(k_3 \text{sig}(\mathcal{E}_p)^{\alpha_3} + k_4 \text{sig}(\mathcal{E}_v)^{\alpha_4} \\ &\quad + k_3 \zeta^p + k_4 \zeta^v) \end{aligned} \tag{31}$$

where $\zeta^p = [(\zeta_1^p)^T, (\zeta_2^p)^T, \dots, (\zeta_M^p)^T]^T$, $\zeta^v = [(\zeta_1^v)^T, (\zeta_2^v)^T, \dots, (\zeta_M^v)^T]^T$.

Moreover, The triggering function for the i th follower is designed as

$$t_i(t) = \left\| k_3 \zeta_i^p(t) \right\| + \left\| k_4 \zeta_i^v(t) \right\| - \eta \left\| \text{sig}(\mathcal{E}_{vi}(t))^{\alpha_4} \right\| \tag{32}$$

where $\eta \in (0, 1)$ is the parameter that can be adjusted. The triggering condition is defined as $t_{k+1}^i = \inf \{ t > t_k^i, t_i(t) > 0 \}$.

Theorem 3 When the Assumption 2 holds, followers use control protocol (27) and distributed triggering function (32), if exists $\vartheta, \kappa > 0$, conditions in Theorem 1 hold and k_3, k_4 satisfy the inequalities (33), (34), all followers can converge to the convex hull spanned by the real leaders in a finite time. Moreover the Zeno behavior of the containment system is excluded.

$$k_3 > 2^{\frac{2(1+\alpha_3)}{3+\alpha_3}} \left(\sqrt{\frac{2}{\lambda_{\min}(L_3)}} \frac{\vartheta \lambda_{\max}(L_3)(1 + \alpha_3)}{3 + \alpha_3} \right)^{1+\alpha_3} (1 + \alpha_3)^{\frac{1-\alpha_3}{3+\alpha_3}} \tag{33}$$

$$\begin{aligned} &\frac{k_4(3 + \alpha_3)}{2(1 + \alpha_3)} \left(1 - 3^{\frac{1-\alpha_2}{2}} \eta \right) \left(\frac{\lambda_{\min}(L_3)}{2} \right)^{\frac{1-\alpha_3}{2(1+\alpha_3)}} \\ &> \vartheta k_4 (3M)^{\frac{1-\alpha_3}{2(1+\alpha_3)}} (\eta + M)^{\frac{\alpha_3 \kappa}{1 + \alpha_3} - \frac{1+\alpha_3}{\alpha_3}} + \vartheta \lambda_{\max}(L_3) \end{aligned} \tag{34}$$

Proof From Theorem 1 and the previous proof, we take the same procedure of the proof for followers, one can prove that under the control protocol (27), \mathcal{E}_p and \mathcal{E}_v can converge to the origin in finite time T_2 . Further to exclude the Zeno behavior, by employing the same procedure of the proof for real leaders in Theorem 2, we can conclude that the inter-event interval has a positive lower bound.

$$\Delta > \frac{3^{\frac{1-\alpha_4}{2}} \eta \|\mathcal{E}_{vi}\|^{\alpha_4}}{2\mu_1 \mu_2} \tag{35}$$

where Δ denotes the inter-event interval, $\mu_1 = \max \left(3^{\frac{1-\alpha_3}{2}} k_3, 3^{\frac{1-\alpha_4}{2}} k_4 \right)$, $\mu_2 = \max \left(\|\mathcal{E}_{vi}(t)\|^{\alpha_3}, \|\dot{\mathcal{E}}_{vi}(t)\|^{\alpha_4} \right)$. This completes the proof. \square

Remark 2 The conclusion of Theorem 3 is established on the basis of Theorem 1. when the real leaders achieve the desired formation, the followers can enter the convex hull generated by the the real leaders and the multi-UAV system (2) eventually accomplish the formation-containment tracking task.

Simulation results

In order to verify the validity and superiority of the proposed method in achieving formation containment tracking, this section uses a scenario containing 7 UAVs to conduct a simulation experiment. The People Computer(PC) is equipped with Intel(R) Core(TM) i5-8300H 2.3GHZ CPU, 8GB memory. Simulations are executed in MATLAB environment. The UAVs in the Multi-UAV system are depicted by the dynamic model (2) with $p_i = [p_{i1}, p_{i2}, p_{i3}]^T$, $v_i = [v_{i1}, v_{i2}, v_{i3}]^T$, $i = 0, 1, \dots, 7$, where p_{i1}, p_{i2} and p_{i3} describe the positions in the directions X, Y and Z, v_{i1}, v_{i2} and v_{i3} are the velocities in X, Y and Z. The Multi-UAV system consists of the guidance UAV denoted by $i = 0$, the outer UAVs represented by index set $E = \{1, 2, 3, 4\}$ and the inner UAVs represented by index set $F = \{5, 6, 7\}$. The information interaction topology between UAVs is shown in Fig. 3. The initial

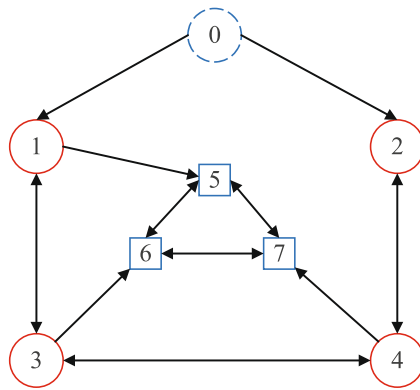


Figure 3. The interaction topology among 7 UAVs.

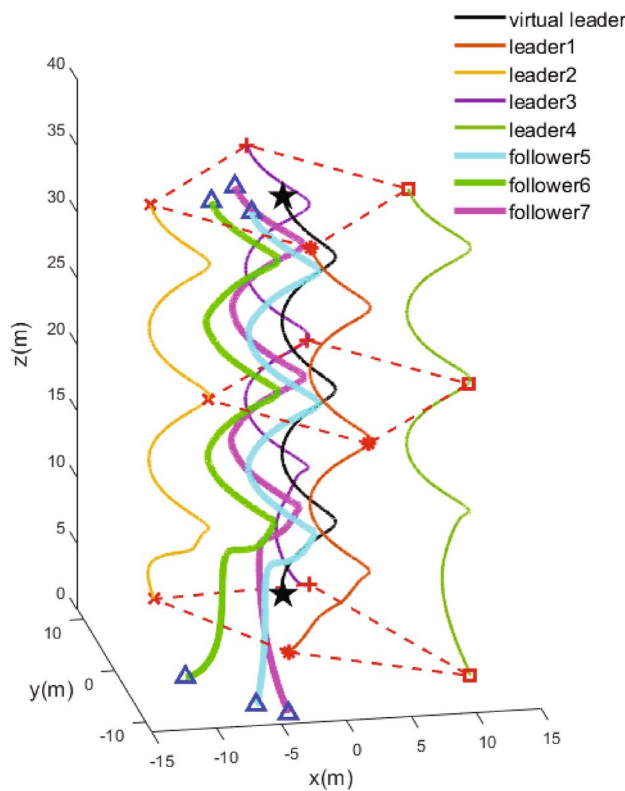


Figure 4. Three dimensional trajectory of UAVs.

state of each agent in the Multi-UAV system is selected as follows: $p_{ij}(0) = 10\Theta$ ($i = 1, 2, 3, 4, 5, 6, 7; j = 1, 2, 3$), $v_{ij}(0) = \Theta$ ($i = 1, 2, 3, 4, 5, 6, 7; j = 1, 2, 3$), where Θ is a random number in the range $(0, 1)$. The guidance and outer UAVs require to accomplish a formation tracking with a square configuration, where the offset vectors are shown as $o_1 = [0, -10, 0]^T$, $o_2 = [-10, 0, 0]^T$, $o_3 = [0, 10, 0]^T$, $o_4 = [10, 0, 0]^T$.

The guidance UAV leads the multi-UAV system with the following desired time-varying reference trajectory:

$$\begin{cases} p_{01} = -2 \cos(0.1\pi t) + 1 \\ p_{02} = 2 \sin(0.1\pi t) \\ p_{03} = 0.5t + 2 \end{cases} \quad (36)$$

The coefficients of observer (5) are chosen as $\alpha = \beta = 5, a = d = 7, b = c = 5$ and the control parameters of protocols (7) and (27) are selected as $k_1 = 4, k_2 = 2, \alpha_1 = 0.7, \alpha_2 = \frac{2\alpha_1}{1+\alpha_1}, k_3 = 6, k_4 = 3, \alpha_3 = 0.8, \alpha_4 = \frac{2\alpha_3}{1+\alpha_3}$. Choose $\xi = 0.5, \eta = 0.8$ as the parameters of the triggering functions (11) and (32). All parameters are the same on all three channels.

The simulation results are demonstrated from Figs. 4, 5, 6, 7, 8 and 9. Figure 4 shows the three-dimensional trajectory of the UAVs. Figure 5 shows the position snapshots of the multi-UAV system at different

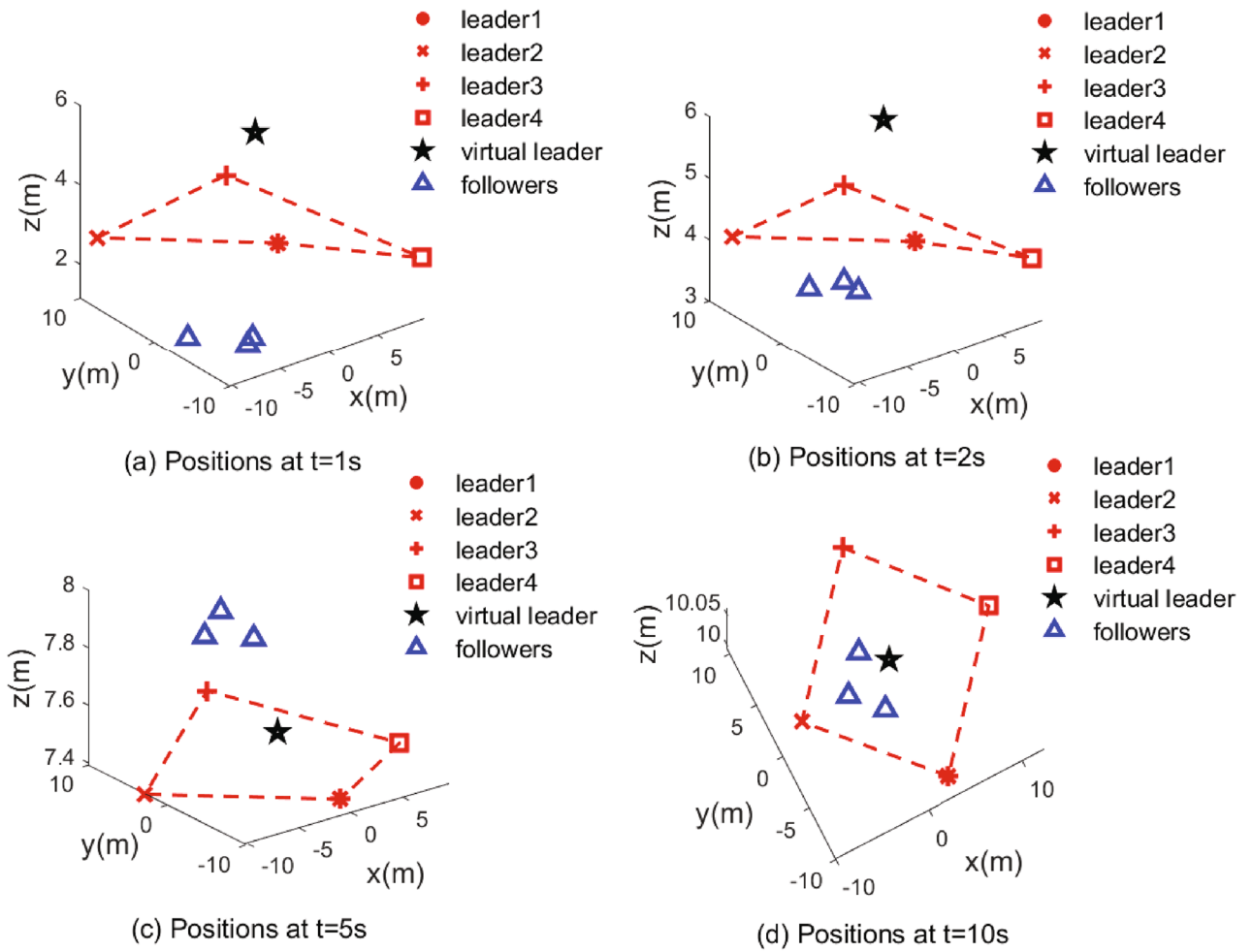


Figure 5. Position snapshots at t = 1 s, 2 s, 5 s, 10 s for the UAVs.

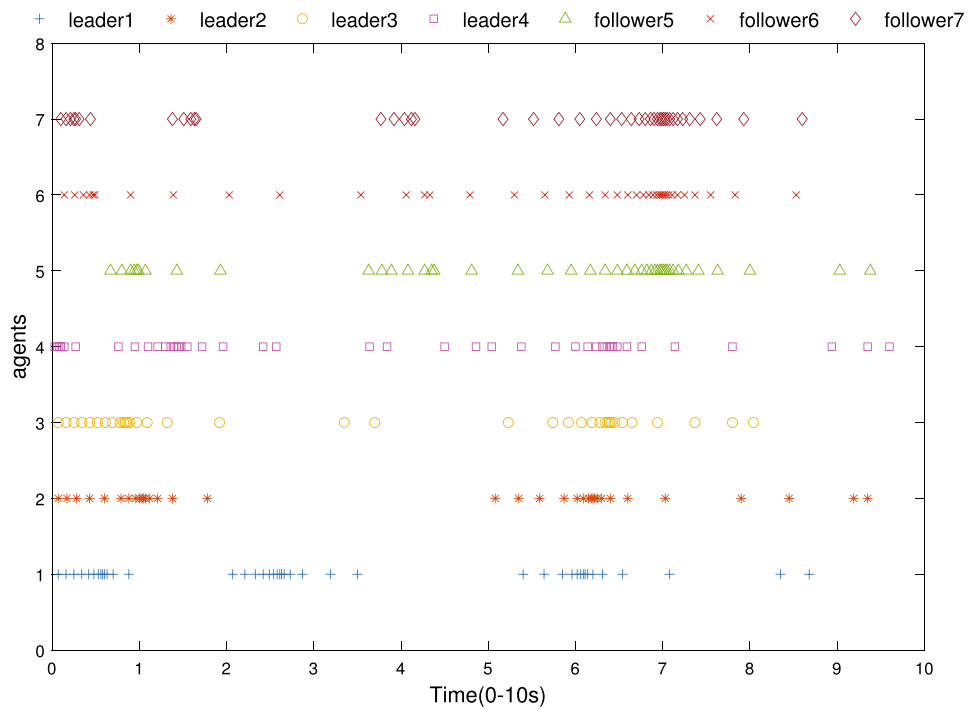


Figure 6. Events triggering times of UAVs.

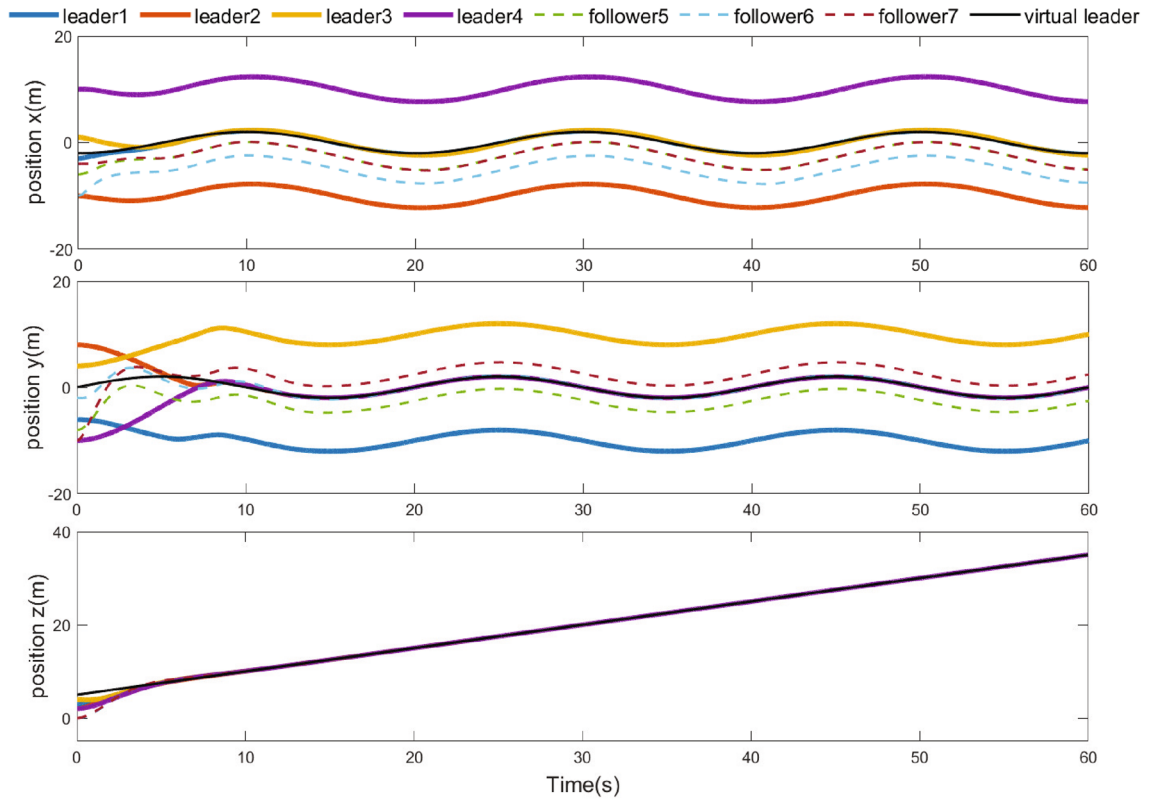


Figure 7. Positions of UAVs.

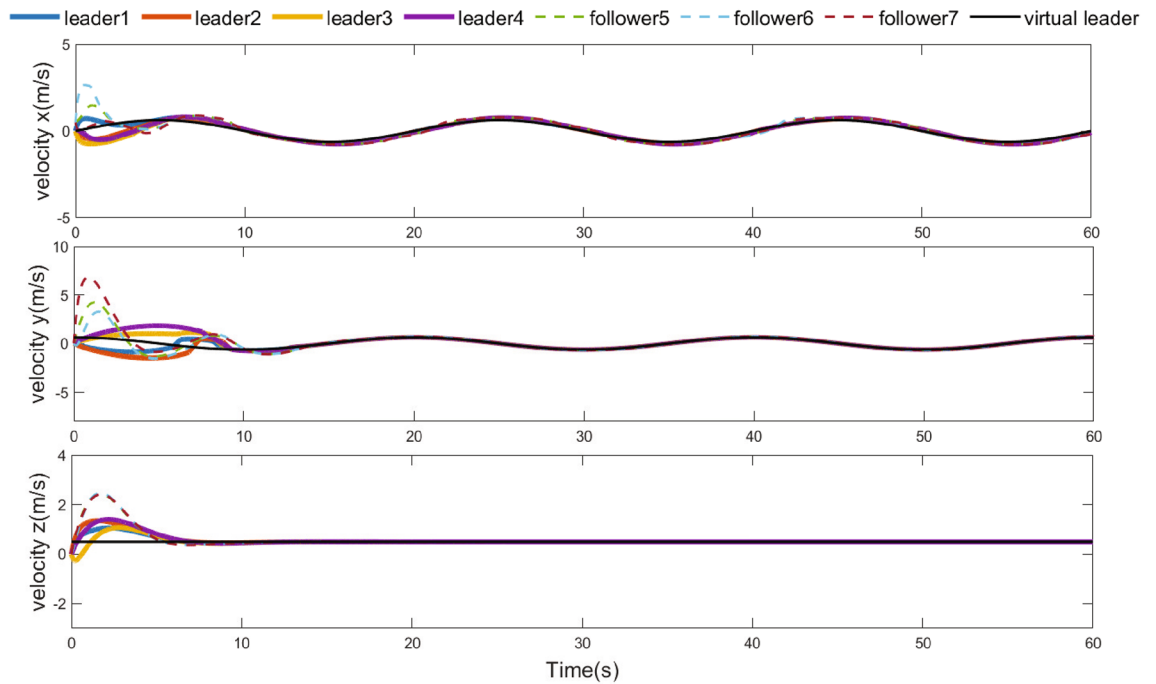


Figure 8. Velocities of UAVs.

times $t=1$ s, 2 s, 5 s and 10 s. Figure 6 gives the events triggering times of 7 UAVs within 10 s. The evolutions of the position and velocity of each UAV in the X, Y and Z directions are given in Figs. 7 and 8. The formation tracking error displayed in Fig. 9a is defined as $\| \Gamma_E \| = \| \Gamma_E \|_1$, with $\Gamma_E = [\Gamma_{E1}, \Gamma_{E2}, \Gamma_{E3}, \Gamma_{E4}]^T$, where

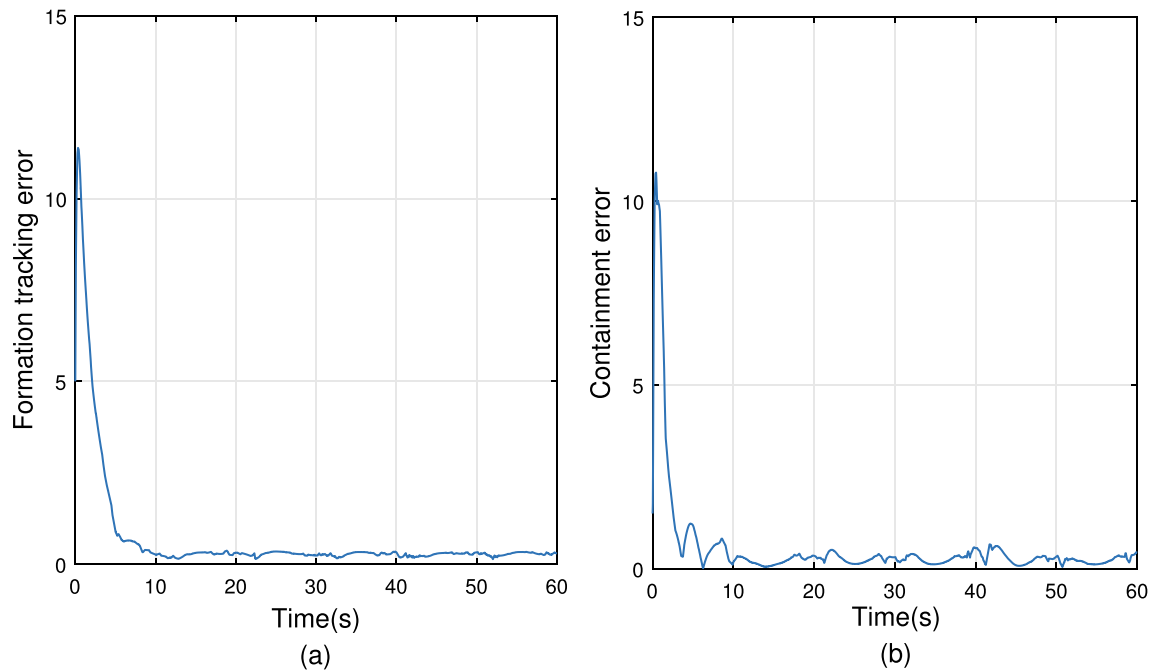


Figure 9. Curves of the formation tracking error for the leaders and the containment error for the followers. (a) Formation tracking error. (b) Containment error.

$\forall i = 1, 2, 3, 4, h_i = [o_i, 0_3]^T$, $\|F_i\| = \|\chi_i - h_i - \chi_0\|_1$. Similarly, the containment error Γ_C is obtained and shown in Fig. 9b.

From Figs. 4, 5, 6, 7, 8 and 9, it can be clearly seen that the outer UAVs achieve the desired formation in a finite time, the inter UAVs enter the convex hull, and the task of formation-containment tracking is accomplished. In addition, with the time-varying of the state of guidance UAV, the multi-UAV system can still realize formation-containment tracking, which shows the robustness of the method proposed in this paper. At the initial time $t=0$, the UAVs are randomly distributed in the space. After 1 s, in order to realize the formation, the outer UAVs start to move. At $t=2$ s, the inner UAVs converge to the convex hull, and at $t=5$ s and at 10 s of the snapshots show that the outer UAVs slowly achieve the square formation around the guidance UAV, and the inner UAVs enter the convex hull formed by the outer UAVs. Figure 6 shows that Zeno behavior does not occur, and the minimum interval of two adjacent events in the leaders' system and followers' system are 0.2 s and 0.4 s respectively, which indicates that the internal communication of the system is intermittent, not continuously. We can also see from Fig. 9 that the systematic error of the UAVs converges to the origin within 10 s. Therefore, under protocols (7) and (27), and with the triggering function satisfying (11) and (32), the multi-UAV system can realize the finite-time event-triggered formation-containment tracking.

Conclusions

In this paper, the problem of time-varying out formation-containment tracking of multi-UAV systems is studied, with a three-layer hierarchical structure being introduced. A finite-time event-triggered control protocol is proposed for real leaders and followers, respectively. The problems of limited communication resources and slow convergence speed in multi-UAV systems are solved at the same time. The simulation results show that the time-varying tracking task can be completed in finite time, and the system does not exist zeno behavior. In future work, we will consider the obstacle avoidance problem in the tracking process, and consider the output saturation of the system to make the system more robust.

Data availability

All data included in this study are available upon request by contact with the corresponding author.

Received: 15 July 2022; Accepted: 9 November 2022

Published online: 24 November 2022

References

- Zhang, X. *et al.* Self-triggered based coordinate control with low communication for tethered multi-UAV collaborative transportation. *IEEE Robot. Autom. Lett.* **6**(2), 1559–1566 (2021).
- Guo, K., Li, X. & Xie, L. Ultra-wideband and odometry-based cooperative relative localization with application to multi-UAV formation control. *IEEE Trans. Cybern.* **50**(6), 2590–2603 (2019).
- Liang, H., Du, Z., Huang, T. & Pan, Y. Neuroadaptive performance guaranteed control for multiagent systems with power integrators and unknown measurement sensitivity. *IEEE Trans. Neural Netw. Learn. Syst.* **20**, 20 (2022).

4. Pan, Y., Li, Q., Liang, H. & Lam, H.-K. A novel mixed control approach for fuzzy systems via membership functions online learning policy. *IEEE Trans. Fuzzy Syst.* **20**, 20 (2021).
5. Li, D., Chen, C. P., Liu, Y.-J. & Tong, S. Neural network controller design for a class of nonlinear delayed systems with time-varying full-state constraints. *IEEE Trans. Neural Netw. Learn. Syst.* **30**(9), 2625–2636 (2019).
6. Kolaric, P., Chen, C., Dalal, A. & Lewis, F. L. Consensus controller for multi-UAV navigation. *Control Theory Technol.* **16**(2), 110–121 (2018).
7. Wang, J., Han, L., Dong, X., Li, Q. & Ren, Z. Distributed sliding mode control for time-varying formation tracking of multi-UAV system with a dynamic leader. *Aerosp. Sci. Technol.* **111**, 106549 (2021).
8. Lei, Y., Wang, Y.-W., Yang, W. & Liu, Z.-W. Distributed control of heterogeneous multi-agent systems with unknown control directions via event/self-triggered communication. *J. Franklin Inst.* **357**(17), 12163–12179 (2020).
9. Liao, R., Han, L., Dong, X., Liu, F., Li, Q., & Ren, Z. Finite-time time-varying formation tracking for second-order multi-agent systems with a leader of fully unknown input. In *2020 39th Chinese Control Conference (CCC)*, pp. 4878–4883. IEEE (2020).
10. Zhang, B., Sun, X., Liu, S. & Deng, X. Adaptive model predictive control with extended state observer for multi-UAV formation flight. *Int. J. Adapt. Control Signal Process.* **34**(10), 1341–1358 (2020).
11. Yu, Z., Liu, Z., Zhang, Y., Qu, Y. & Su, C.-Y. Distributed finite-time fault-tolerant containment control for multiple unmanned aerial vehicles. *IEEE Trans. Neural Netw. Learn. Syst.* **31**(6), 2077–2091 (2019).
12. Chen, L., Li, C., Sun, Y. & Ma, G. Distributed finite-time containment control for multiple Euler–Lagrange systems with communication delays. *Int. J. Robust Nonlinear Control* **29**(1), 332–352 (2019).
13. Das, A. K. *et al.* A vision-based formation control framework. *IEEE Trans. Robot. Autom.* **18**(5), 813–825 (2002).
14. Fax, J. A. & Murray, R. M. Information flow and cooperative control of vehicle formations. *IEEE Trans. Autom. Control* **49**(9), 1465–1476 (2004).
15. Ge, S. S., Liu, X., Goh, C.-H. & Xu, L. Formation tracking control of multiagents in constrained space. *IEEE Trans. Control Syst. Technol.* **24**(3), 992–1003 (2015).
16. Ma, Q. & Miao, G. Distributed containment control of linear multi-agent systems. *Neurocomputing* **133**, 399–403 (2014).
17. Biao, T., Xingling, S., Wei, Y. & Wendong, Z. Fixed time output feedback containment for uncertain nonlinear multiagent systems with switching communication topologies. *ISA Trans.* **111**, 82–95 (2021).
18. Haghshenas, H., Badamchizadeh, M. A. & Baradarannia, M. Containment control of heterogeneous linear multi-agent systems. *Automatica* **54**, 210–216 (2015).
19. Liu, S., Xie, L. & Zhang, H. Containment control of multi-agent systems by exploiting the control inputs of neighbors. *Int. J. Robust Nonlinear Control* **24**(17), 2803–2818 (2014).
20. Han, L., Dong, X., Li, Q. & Ren, Z. Formation-containment control for second-order multi-agent systems with time-varying delays. *Neurocomputing* **218**, 439–447 (2016).
21. Dong, X., Li, Q., Ren, Z. & Zhong, Y. Formation-containment control for high-order linear time-invariant multi-agent systems with time delays. *J. Franklin Inst.* **352**(9), 3564–3584 (2015).
22. Wang, Y., Song, Y. & Ren, W. Distributed adaptive finite-time approach for formation-containment control of networked nonlinear systems under directed topology. *IEEE Trans. Neural Netw. Learn. Syst.* **29**(7), 3164–3175 (2017).
23. Hua, Y., Dong, X., Li, Q., & Ren, Z. Formation-containment tracking for high-order linear multi-agent systems on directed graphs. In *IECON 2017-43rd Annual Conference of the IEEE Industrial Electronics Society*, pp. 5809–5814. IEEE (2017).
24. Hua, Y., Dong, X., Han, L., Li, Q. & Ren, Z. Formation-containment tracking for general linear multi-agent systems with a tracking-leader of unknown control input. *Syst. Control Lett.* **122**, 67–76 (2018).
25. Zhang, Y., Wen, Y., Chen, G. & Chen, Y.-Y. Distributed adaptive observer-based output formation-containment control for heterogeneous multi-agent systems with unknown inputs. *IET Control Theory Appl.* **14**(15), 2205–2212 (2020).
26. Hua, Y., Dong, X., Han, L., Li, Q. & Ren, Z. Finite-time time-varying formation tracking for high-order multiagent systems with mismatched disturbances. *IEEE Trans. Syst. Man Cybern. Syst.* **50**(10), 3795–3803 (2018).
27. Pan, Y., Wu, Y. & Lam, H.-K. Security-based fuzzy control for nonlinear networked control systems with dos attacks via a resilient event-triggered scheme. *IEEE Trans. Fuzzy Syst.* **20**, 1 (2022).
28. Lei, Y., Wang, Y.-W., Morarescu, I.-C. & Postoyan, R. Event-triggered fixed-time stabilization of two-time-scale linear systems. *IEEE Trans. Autom. Control* **20**, 20 (2022).
29. Lei, Y., Wang, Y.-W., Liu, X.-K. & Liu, Z.-W. Distributed event-triggered synchronization of interconnected linear two-time-scale systems with switching topology. *IEEE Trans. Cybern.* **20**, 20 (2021).
30. Chen, L., Li, C., Xiao, B. & Guo, Y. Formation-containment control of networked Euler–Lagrange systems: An event-triggered framework. *ISA Trans.* **86**, 87–97 (2019).
31. Wei, L., Chen, M. & Li, T. Dynamic event-triggered cooperative formation control for UAVs subject to time-varying disturbances. *IET Control Theory Appl.* **14**(17), 2514–2525 (2020).
32. Sun, C., Hu, G., Xie, L. & Egerstedt, M. Robust finite-time connectivity preserving coordination of second-order multi-agent systems. *Automatica* **89**, 21–27 (2018).
33. Zhang, A., Zhou, D., Yang, P. & Yang, M. Event-triggered finite-time consensus with fully continuous communication free for second-order multi-agent systems. *Int. J. Control Autom. Syst.* **17**(4), 836–846 (2019).
34. Bhat, S. P. & Bernstein, D. S. Finite-time stability of continuous autonomous systems. *SIAM J. Control. Optim.* **38**(3), 751–766 (2000).
35. Zhou, S., Guo, K., Yu, X., Guo, L. & Xie, L. Fixed-time observer based safety control for a quadrotor UAV. *IEEE Trans. Aerosp. Electron. Syst.* **57**(5), 2815–2825 (2021).
36. Dong, X., Zhou, Y., Ren, Z. & Zhong, Y. Time-varying formation control for unmanned aerial vehicles with switching interaction topologies. *Control. Eng. Pract.* **46**, 26–36 (2016).
37. Hassan, M. F. & Hammuda, M. Leader-follower formation control of mobile nonholonomic robots via a new observer-based controller. *Int. J. Syst. Sci.* **51**(7), 1243–1265 (2020).

Author contributions

X.C.:wrote the main manuscript text. X.Z.:simulations in Matlab. W.Y.: validation simulations in Matlab. All authors contributed to the article and approved the submitted version.

Funding

This research was funded by National Natural Science Foundation of China, grant number 11725211.

Competing interests

The authors declare no competing interests.

Additional information

Correspondence and requests for materials should be addressed to W.Y.

Reprints and permissions information is available at www.nature.com/reprints.

Publisher's note Springer Nature remains neutral with regard to jurisdictional claims in published maps and institutional affiliations.



Open Access This article is licensed under a Creative Commons Attribution 4.0 International License, which permits use, sharing, adaptation, distribution and reproduction in any medium or format, as long as you give appropriate credit to the original author(s) and the source, provide a link to the Creative Commons licence, and indicate if changes were made. The images or other third party material in this article are included in the article's Creative Commons licence, unless indicated otherwise in a credit line to the material. If material is not included in the article's Creative Commons licence and your intended use is not permitted by statutory regulation or exceeds the permitted use, you will need to obtain permission directly from the copyright holder. To view a copy of this licence, visit <http://creativecommons.org/licenses/by/4.0/>.

© The Author(s) 2022